IOP Conf. Series: Materials Science and Engineering **201** (2017) 012050 doi:10.1088/1757-899X/201/1/012050

Facile synthesis of cupric hydroxide and cupric oxide on copper foil for potential electrochemical applications

E M A Espejo[1], **M D L Balela**[2]

Sustainable Electronic Materials Group, Department of Mining, Metallurgical, and Materials Engineering, University of the Philippines Diliman, Quezon City 1101, Philippines

[1]erikamaeespejo@gmail.com, [2]mlbalela1@up.edu.ph

Abstract. This paper presents the synthesis of cupric hydroxide [$Cu(OH)_2$] and cupric oxide (CuO) *via* a simple *in situ* oxidation of copper (Cu) foil in alkaline solution for electrode materials in pseudocapacitors. $Cu(OH)_2$ and $Cu(OH)_2$/CuO film grown on Cu substrate offer binderless and additive-free active materials directly in contact with the current collector. This approach allows more efficient interaction of electrolyte and the active material in terms of charge and mass exchange for higher capacitance. The Cu-based nanomaterials have uniform morphology, and are needle-like and flower-like in structure for $Cu(OH)_2$ and $Cu(OH)_2$/CuO, respectively. The fabricated nanostructures exhibit a specific capacitance in the range of 400–2000 F/g.

1. Introduction

Research on efficient, clean, sustainable, and renewable energy sources has been on the rise due to carbon emission, exhaustion of fossil fuels, and increase in environmental pollution [1–8]. However, clean energy research can only progress with the simultaneous development of efficient energy storage systems.

Supercapacitors are energy devices which have high power density, operating safety, environment benignity, fast charging/discharging rate, long-term cycle stability, high energy density, faster response time and near-infinite life cycle [1–8]. They are classified into two types, namely electric double-layer capacitors (EDLCs) and pseudocapacitors. In EDLCs, charge/energy storage takes place through ion adsorption/desorption at the electrode–electrolyte interface [1]. The process is non-Faradaic; no electron transfer takes place across the electrode interface and the storage of electric charge and energy is electrostatic. However, EDLCs have limited specific capacitance due to their double-layer charge storage mechanism [2].

Pseudocapacitors, on the other hand, store energy by Faradaic battery-type oxidation–reduction reactions leading to their pseudocapacitive behavior wherein the electrical charge can be built up *via* electron transfer that produces the changes in the chemical or oxidization state of the electrochemically active materials [1, 2].

Transition metal hydroxides and oxides have been explored as electrode materials of pseudocapacitors to increase the capacitance due to their nanostructures which can store charges for long periods of time without appreciable leakage, making them suitable for electrochemical

applications [1, 3]. In particular, metal hydroxides and oxides have received significant attention due to their cost-effective characteristics. Cupric hydroxides and oxides are promising materials for pseudocapacitors in view of their abundance, low cost, environmental friendly nature and high specific capacitance of 100–800 F/g [2, 3, 4, 5, 6, 9]. In addition, copper compounds can exhibit numerous nanostructures which is advantageous for energy storage [4].

Herein, the morphology and properties of $Cu(OH)_2$ and $Cu(OH)_2$/CuO nanostructures fabricated on Cu foil *via* a simple, binderless, and additive-free liquid–solid reaction are presented. Oxidation was performed by immersing the Cu foil in NaOH/$(NH_4)_2S_2O_8$ aqueous solution. Such a facile approach to growing various oxide nanostructures using water has been applied to ZnO, resulting in hierarchical structures of nanorods, nanotubes and nanoflowers [10]. The effect of reaction time on the morphology, phase composition and crystal structure of the resulting Cu compound was investigated by scanning electron microscopy (SEM) and X-ray diffraction (XRD). Additionally, the electrochemical properties was studied by cyclic voltammetry.

2. Experimental

All chemicals used were of analytical grade and used as received without further purification. In a typical experiment, 1 × 1 cm^2 pieces of copper foil were ultrasonically cleaned in acetone, ethanol, and deionized water consecutively for 10 min. The copper substrates were then immersed in 1 M HCl solution to remove other oxides and impurities. The pre-cleaned Cu foils were then dried in air and nail enamel was used to cover one side of the substrates. To fabricate the copper compounds, the substrates were immersed in a solution containing 12 mL of 10 M NaOH, 6 mL of 1 M $(NH_4)_2S_2O_8$, and 27 mL of deionized water for 30 to 60 min. The substrates were then rinsed with ethanol and deionized water, followed by air drying. The morphology of the Cu products was investigated in a scanning electron microscope (SEM, JEOL Ltd., JSM-5310). The phase composition and crystal structure were also examined by X-ray diffraction (Shimadzu MAXima XRD-7000, Cu K radiation, λ = 0.1542 nm, 30 mA). Cyclic voltammetry was performed using the oxidized Cu substrate, Pt sheet, and silver/silver chloride (Ag/AgCl in 3.5 M KCl, Horiba) as the working, counter and reference electrode, respectively. Measurement was performed in 6 M potassium hydroxide (KOH) aqueous solution at scan rate of 2 mV.

3. Results and discussion

Figure 1 shows the optical images of the Cu foil before and after oxidation in NaOH/$(NH_4)_2S_2O_8$ aqueous solution for 30–60 min. The pre-cleaned Cu foil appeared darker brown in color compared to the sample after cleaning in HCl, which can be attributed to surface oxides and other impurities. After 30 min of reaction in NaOH/$(NH_4)_2S_2O_8$ aqueous solution, the Cu foil changed from rose gold to blue, which possibly indicates the formation of Cu compound on the surface. Prolonged reaction to 60 min resulted in the blackening of some areas of the blue Cu film. This suggests the presence of a different Cu compound.

Figure 1. Optical images of (a) pre-cleaned and cleaned Cu foil (b) before and after oxidation in NaOH/$(NH_4)_2S_2O_8$ aqueous solution for (c) 30 and (d) 60 min at room temperature.

Figure 2 shows the corresponding XRD patterns of cleaned Cu foil after immersion in NaOH/$(NH_4)_2S_2O_8$ aqueous solution for 30–60 min. Three peaks at 2θ values of 43.54°, 50.66°, and 74.48° corresponding to the (111), (200), and (220) planes of Cu were observed in both Cu products

(JCPDS file no. 04–0836). In figure 2b, the diffraction peaks at the 2θ values of 16.92°, 24.1°, 34.34°, 36.12°, 38.78°, 40.02°, and 53.58° can be indexed to the (020), (021), (002), (111), (022), (130), and (150) planes of orthorhombic $Cu(OH)_2$, respectively (JCPDS file no. 80-0656). The diffraction peaks corresponding to the (111) and (200) planes of CuO were observed at 2θ values of 35.74° and 38.84° in figure 2a (JCPDS file no. 80-1916). The peaks corresponding to the (130) and (150) planes of $Cu(OH)_2$ were also observed in figure 2b at 2θ values of 40.46° and 53.6°, respectively. This shows that the change in color from blue to black of the Cu film observed in figure 1 could be due to the formation of CuO when the reaction was prolonged to 60 min.

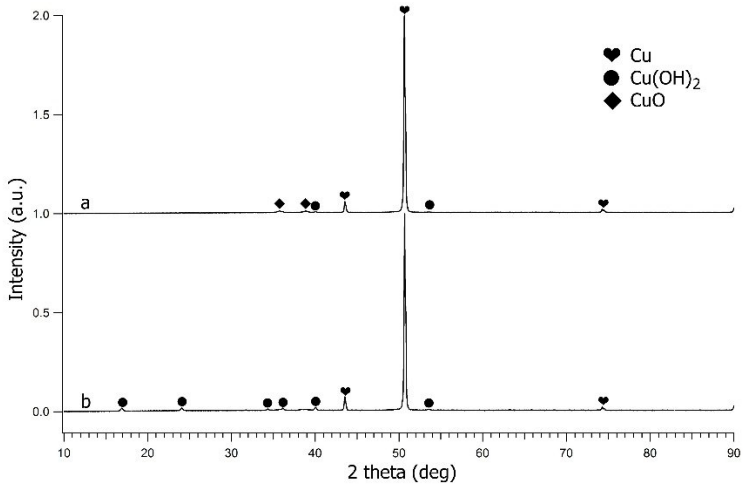

Figure 2. XRD patterns of cleaned Cu foil after immersion in $NaOH/(NH_4)_2S_2O_8$ aqueous solution for (a) 60 and (b) 30 min at room temperature.

Figure 3 shows the SEM images of the Cu products after oxidation in $NaOH/(NH_4)_2S_2O_8$ aqueous solution at room temperature. The $Cu(OH)_2$ film formed after 30 min of reaction exhibits a needle-like structure with a typical length of about 5 µm and width of 200–300 nm as shown in figures 3a–c. On the other hand, microflowers with a diameter of about 3–5 µm mixed together with $Cu(OH)_2$ needles are seen in figures 3d–f. The microflowers possibly correspond to CuO, which explains the observed change in color of some areas of the film from blue to black and the appearance of CuO peaks in the XRD pattern as shown in figure 2a.

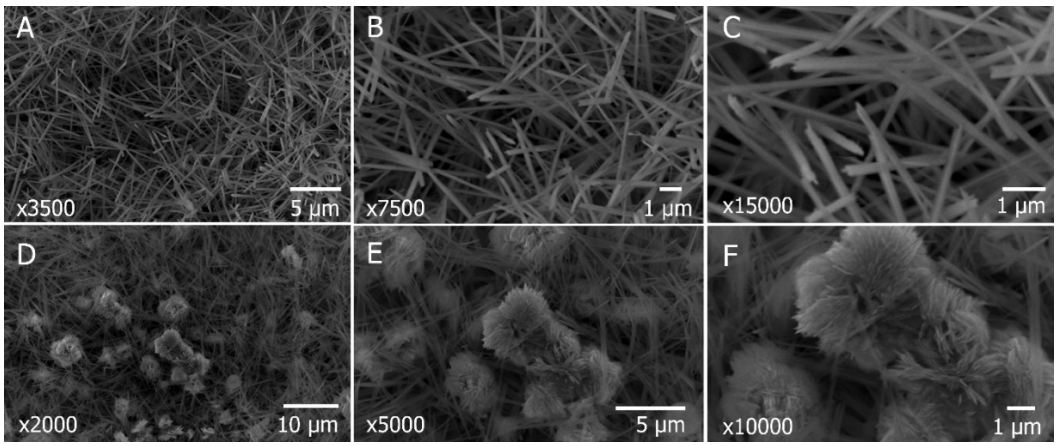

Figure 3. SEM images of cleaned Cu foil after immersion in $NaOH/(NH_4)_2S_2O_8$ aqueous solution for (a–c) 30 and (d–f) 60 min at room temperature.

The formation of $Cu(OH)_2$ and $Cu(OH)_2$/CuO on Cu foil by oxidation of Cu foil in alkaline solution can be understood from the equations below. At 30 min, the growth of $Cu(OH)_2$ on Cu foil is due to the redox reaction between Cu and persulfate ($S_2O_8^{2-}$) forming Cu^{2+} and sulfate (SO_4^{2-}) as shown in equation (1). Cu^{2+} and OH^- then generate μ4–OH bridges, which accompany the nucleation process and formation of $Cu(OH)_2$ [7].

$$2Cu + 8NaOH + 4(NH_4)_2S_2O_8 \rightarrow 2Cu(OH)_2 + 4Na_2SO_4 + 4NH_3 \uparrow + 4H_2O \quad (1)$$

With increasing reaction time, some of the $Cu(OH)_2$ needles are split into nanopieces of CuO sheets and partially form the flower-like structure [7]. Equation (2) shows that CuO are produced due to the hydrogen linkage being unstable under oxidative conditions resulting in removal of water.

$$Cu(OH)_2 \rightarrow CuO + H_2O \quad (2)$$

The change in color of the Cu foil at 60 min reaction time and the mix of $Cu(OH)_2$ needles and CuO flowers in the SEM images in figures 3d–f can be explained by equation (3) wherein the some of the $Cu(OH)_2$ produced at 30 min by equation (1) are converted to CuO by equation (2).

$$2Cu + 8NaOH + 4(NH_4)_2S_2O_8 \rightarrow Cu(OH)_2 + CuO + 4Na_2SO_4 + 4NH_3 \uparrow + 5H_2O \quad (3)$$

Transition metal oxides/hydroxides usually have relatively low power density and poor cycling stability, and the low power density can be ascribed to the poor electric conductivity of metal oxides/hydroxides, which confines electron transfer rates. However, combining metal oxides/hydroxides with conductive materials and developing porous nanostructures can accelerate the reaction kinetics and provide more ion adsorption or active sites for charge transfer reactions as well as shorten the diffusion and transfer pathways of electrolyte ions [11]. The specific capacitance values of some oxide/hydroxide pseudocapacitors have been close to or higher than their theoretical Faradic capacitances, *e.g.* >1000 F/g [3]. Figure 4 shows the CV profiles of the Cu products at a scan rate of 2 mV/s. The specific capacitance of $Cu(OH)_2$ and $Cu(OH)_2$/CuO are 2136 F/g and 422 F/g, respectively based on equation (4):

$$C_s = \frac{1}{mv(E_2 - E_1)} \int_{E_2}^{E_2} i(E)dE \quad (4)$$

where C_s is the specific capacitance, m is the mass loading, v is the scan rate, and E_2 to E_1 is the potential window. Results show that the Cu product obtained after 30 min reaction time displayed higher capacitance.

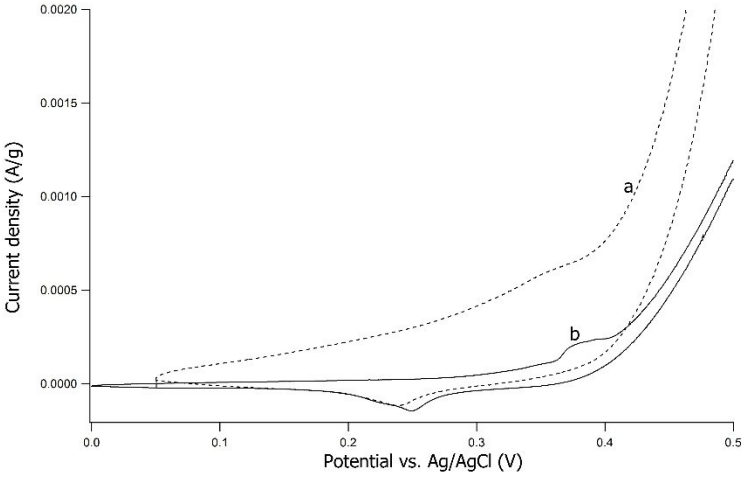

Figure 4. CV curves of the cleaned Cu foil after immersion in $NaOH/(NH_4)_2S_2O_8$ aqueous solution for (a) 30 and (b) 60 min at room temperature.

The cross needle-like architecture of $Cu(OH)_2$ grown on Cu foil provides larger electrode–electrolyte interface, thus good electrical conductivity, and have effective electrolyte-accessible channels for ion transportation and efficient redox reaction compared to CuO flowers [8]. Moreover, the needles are interconnected with each other and create pores and crevices which make a large surface area for easy diffusion of the electrolyte onto the area [9]. These resulted in the high capacitive performance observed from $Cu(OH)_2$.

2D and 3D solids can also have possible applications in pseudocapacitors as their layered structure permits the ionic or neutral species in the electrolyte to intercalate and interact with it [4]. The increase in granular size from needles to flowers may increase the active surface area and hence improve the material's electrochemical properties [12]. However, since one-dimensional morphologies like needles and rods possess the property of directional charge transport, the needle-like $Cu(OH)_2$ displays lower charge transfer resistance and smaller IR drop than the flower-like CuO which greatly enhanced its capacitive performance [2].

Energy stored in a pseudocapacitor is affected by the surface area, structure, particle size, and crystallinity of the material [4]. Therefore, utilizing nanostructured materials is of great importance in this field [8]. The fabricated needle-like $Cu(OH)_2$ and flower-like CuO mixed with $Cu(OH)_2$ microneedles on Cu foil showed high capacitive performance which presents them as potential electrode materials for pseudocapacitors.

4. Conclusion

In summary, needle-like $Cu(OH)_2$ and flower-like CuO mixed with $Cu(OH)_2$ microneedles were successfully fabricated on the surface of Cu foil by a facile oxidation reaction in alkaline solution. The synthesis was a cost-effective one-step method wherein binderless and additive-free materials were obtained. The synthesized copper compounds have unique nanostructures which enable easy interaction with the electrolyte resulting in a specific capacitance of 2136 F/g and 422 F/g for $Cu(OH)_2$ and $CuO/Cu(OH)_2$, respectively.

5. Acknowledgments

This work is supported by the National Research Council of the Philippines under the project "Electrochemical Investigation of the Pseudocapacitive Properties of Ni/NiO Nanowire Nonwoven Electrode Formed Under External Magnetic Field." Project start date: 1 June 2016.

References

[1] Yin B, Zhang S, Zheng X, Qu F and Wu X 2014 *Nano-Micro Lett*. **6** 340–6
[2] Xu P, Ye K, Du M, Lui J, Cheng K, Yin J, Wang G and Cao D 2015 *RSC Adv*. **5** 36656–64
[3] Chen K, Song S, Li K and Xue D 2013 *CrystEngComm* **15** 10367–73
[4] Nwanya A, Obi D, Ozoemena K, Osuji R, Awada C, Ruediger A, Maaza M, Rosei F, Ezema F 2016 *Electrochim. Acta* **198** 220–30
[5] Pendashteh A, Rahmanifar M, Mousavi M F 2014 *Ultrason. Sonochem.* **21** 643–52
[6] Hsu Y-K, Chen Y-C, Lin Y-G 2014 *Electrochim. Acta* **139** 401–7
[7] Liu Y, Qioa Y, Zhang W, Hu P, Chen C, Li Z, Yuan L, Hu Xianluo and Huang Y 2014 *J. Alloys Compd.* **586** 208–15
[8] Ghadge T, Lokhande B J 2016 *J. Mater. Sci.* **51** 9879–88
[9] Lamberti A, Fontana M, Bianco S, Tresso E 2016 *Int. J. Hydrogen Energy* **41** 11700–8
[10] Balela M D L, Pelicano C M O and Lockman Z 2017 *J. Mater. Sci.* **52** 2319–28
[11] Shi F, Li L, Wand X-L, Gu C-D and Tu J-P 2014 *RSC Adv.* **4** 41910–21
[12] Endut Z, Hamdi M, Basirub W J 2013 *Thin Solid Films* **528** 213–16